



Slope and equilibrium: A parsimonious and flexible approach to model microclimate

Eva Gril, Fabien Spicher, Caroline Greiser, Michael B Ashcroft, Sylvain Pincebourde, Sylvie Durrieu, Manuel Nicolas, Benoit Richard, Guillaume Decocq, Ronan Marrec, et al.

► To cite this version:

Eva Gril, Fabien Spicher, Caroline Greiser, Michael B Ashcroft, Sylvain Pincebourde, et al.. Slope and equilibrium: A parsimonious and flexible approach to model microclimate. *Methods in Ecology and Evolution*, 2023, 14 (3), pp.885-897. 10.1111/2041-210x.14048 . hal-04023168

HAL Id: hal-04023168

<https://hal.inrae.fr/hal-04023168>

Submitted on 10 Mar 2023

HAL is a multi-disciplinary open access archive for the deposit and dissemination of scientific research documents, whether they are published or not. The documents may come from teaching and research institutions in France or abroad, or from public or private research centers.












L'archive ouverte pluridisciplinaire **HAL**, est destinée au dépôt et à la diffusion de documents scientifiques de niveau recherche, publiés ou non, émanant des établissements d'enseignement et de recherche français ou étrangers, des laboratoires publics ou privés.



Distributed under a Creative Commons Attribution - NonCommercial 4.0 International License

RESEARCH ARTICLE

Slope and equilibrium: A parsimonious and flexible approach to model microclimate

Eva Gril¹  | Fabien Spicher¹  | Caroline Greiser²  | Michael B. Ashcroft³  |
Sylvain Pincebourde⁴  | Sylvie Durrieu⁵  | Manuel Nicolas⁶  | Benoit Richard¹  |
Guillaume Decocq¹  | Ronan Marrec¹  | Jonathan Lenoir¹ 

¹UMR CNRS 7058 "Ecologie et Dynamique des Systèmes Anthropisés" (EDYSAN), Université de Picardie Jules Verne, Amiens, France; ²Department of Physical Geography and Bolin Centre for Climate Research, Stockholm University, Stockholm, Sweden; ³Centre for Sustainable Ecosystem Solutions, School of Earth, Atmospheric and Life Sciences, University of Wollongong, Wollongong, New South Wales, Australia; ⁴Institut de Recherche sur la Biologie de l'Insecte, UMR 7261, CNRS, Université de Tours, Tours, France; ⁵UMR Territoires, Environnement, Télédétection et Information Spatiale (TETIS), INRAE, AgroParisTech, CIRAD, CNRS, Univ Montpellier, Montpellier, France and ⁶Département Recherche et Développement, Office National des Forêts, Fontainebleau, France

Correspondence

Eva Gril

Email: eva.gril@u-picardie.fr

Funding information

Agence Nationale de la Recherche, Grant/Award Number: N°ANR-19-CE32-0005-01: IMPRINT; Centre National de la Recherche Scientifique, Grant/Award Number: Défi INFINITI 2018: MORFO

Handling Editor: Nick Isaac

Abstract

1. Most statistical models of microclimate focus on the difference or 'offset' between standardized air temperatures (macroclimate) and those of a specific habitat such as forest understorey, grassland or under a log. However, these offsets can fluctuate from positive to negative over a single day such that common practice consists in aggregating data into daily mean, minimum and maximum before modelling monthly offsets for each summary statistic. Here, we propose a more parsimonious and flexible approach relying on just two parameters: the slope and equilibrium. The slope captures the linear relationship between microclimate and macroclimate, while the equilibrium is the point at which microclimate equals macroclimate. Although applicable to other habitats, we demonstrate the relevance of our method by focusing on forest understoreys.
2. We installed temperature sensors at 1-m height inside forest stands and in nearby open grasslands equipped with standardized weather stations, across 13 sites in France spanning a wide climatic gradient. From a year of hourly temperatures and for each sensor, we established relationships between microclimate and macroclimate temperatures using two linear mixed-effects models, during the leaf-on (May–November) and leaf-off period (December–April). We extracted the monthly equilibrium and slope for each sensor, and used another set of linear mixed-effects models to investigate their main determinants.
3. The slope was chiefly determined by stand structure variables interacting with the leaf-on/leaf-off period: stand type (conifer vs broadleaf); shade-casting ability; stand age; dominant height; stem density; and cover of the upper and lower shrub layer. In contrast, forest structure had no explanatory power on the

This is an open access article under the terms of the [Creative Commons Attribution-NonCommercial](https://creativecommons.org/licenses/by-nc/4.0/) License, which permits use, distribution and reproduction in any medium, provided the original work is properly cited and is not used for commercial purposes.

© 2022 The Authors. *Methods in Ecology and Evolution* published by John Wiley & Sons Ltd on behalf of British Ecological Society.

equilibrium. We found the equilibrium to be positively related to mean macroclimate temperature, interacting with the open/forest habitat.

4. The method introduced here overcomes several shortcomings of modelling microclimate offsets. By demonstrating that the slope and equilibrium vary in predictable ways, we have established a general linkage between microclimate and macroclimate temperatures that can be applied to any location or time if we know the mean macroclimate temperature (equilibrium) and buffering or amplifying capacity of the habitat (slope). We also warn about methodological biases due to the reference used for macroclimate.

KEYWORDS

buffering, canopy cover, forest, macroclimate, microclimate, offset, temperature sensor, weather station

1 | INTRODUCTION

Scientists have been discussing the impacts of temperature on biodiversity for centuries (Humboldt & Bonpland, 1805), but the ongoing global warming crisis has made it a central concern (Lenoir et al., 2020). Ecological studies usually rely on gridded temperature maps from large-scale datasets such as WorldClim (Fick & Hijmans, 2017) or ERA5-Land (Muñoz-Sabater et al., 2021). These 'macroclimate' maps are interpolated from weather stations, systematically located in fully exposed areas, following official recommendations from the World Meteorological Organization (WMO, 2018), and are provided at coarse spatial resolutions (1–9 km), hiding important fine-scale (centimetres to metres) microclimate variation (Lembrechts et al., 2019).

Many species, in fact, experience temperature regimes vastly different from those measured by weather stations and predicted by macroclimate maps (Potter et al., 2013). Some species live in habitats that are buffered from temperature extremes (Figure 1a,c), such as those living beneath the soil surface, under water or snow, in termite mounds or forest understoreys (De Frenne et al., 2021; Woods et al., 2021). Indeed, temperature is often buffered beneath forest canopies, thanks to the shading and transpiration provided by trees and shrubs (Geiger et al., 2003). Conversely, plants in an open grassland, insects on exposed leaves or ants living on the soil surface could experience daily maximum temperatures up to 20°C higher than macroclimate air temperatures (Miller et al., 2021; Pincebourde & Suppo, 2016) as well as colder minimum temperatures and even frosts, which suggests amplified fluctuations, or swings in temperature over time (Figure 1b,d).

The development of temperature sensors over the last decade has greatly improved our understanding of spatiotemporal variability in microclimate temperatures (Bramer et al., 2018), as well as our ability to predict local conditions from macroclimate data (Lembrechts et al., 2019). Mechanistic models computing heat transfers are a powerful approach to estimate microclimate temperature (Kearney et al., 2020), but they require extensive parameterization, with specific sets of parameters for different habitats. Statistical

models usually focus on offsets (i.e. microclimate minus macroclimate temperatures), rather than the actual value of microclimate temperature (Zellweger et al., 2019). This approach has proved fruitful, as demonstrated for instance by Haesen et al. (2021) who generated maps of European forest temperature at 25-m resolution, using global macroclimate maps and spatially interpolated offsets. However, offsets are far from constant over time, and can swing from positive to negative according to the time of day (De Frenne et al., 2021). Common practice consists of aggregating temperature records into daily summary statistics (mean, minimum and maximum) before computing monthly averages (e.g. Frey et al., 2016; Haesen et al., 2021). This may result in up to 36 different models for monthly mean, minimum and maximum temperatures; without the possibility to use the full statistical power of the raw data, usually hourly, or to refine predictions to the initial temporal resolution.

Here, we propose a hybrid, more parsimonious and flexible approach relying on just two synthetic parameters: the slope and equilibrium. The slope is the coefficient of the linear relationship between microclimate and macroclimate, while the equilibrium is the point at which macroclimate equals microclimate (De Frenne et al., 2021). A slope value close to one suggests a tight coupling, while a slope value lower or greater than 1 means pronounced microclimatic processes, respectively, buffering or amplifying the macroclimate variability (Figure 1). The slope parameter has already been considered as a key mechanistic parameter to capture microclimate dynamics for temperature (Lenoir et al., 2017; Locosselli et al., 2016; Rita et al., 2021) or other climatic factors like vapour pressure deficit (Davis, Dobrowski, et al., 2019). The equilibrium, unlike the classical y-axis intercept from a linear model, also has a biophysical meaning since it represents the mean climatic condition (here temperature) for which the habitat has an imperceptible effect on microclimate. Large radiative fluxes exacerbate microclimatic differences, for instance between open and closed-canopy habitats. In their absence—that is, during wet, cloudy days—a 'mild' temperature is expected inside and outside of the habitat, flattening out any microclimatic differences and thus being closer to the equilibrium. This equilibrium is likely to

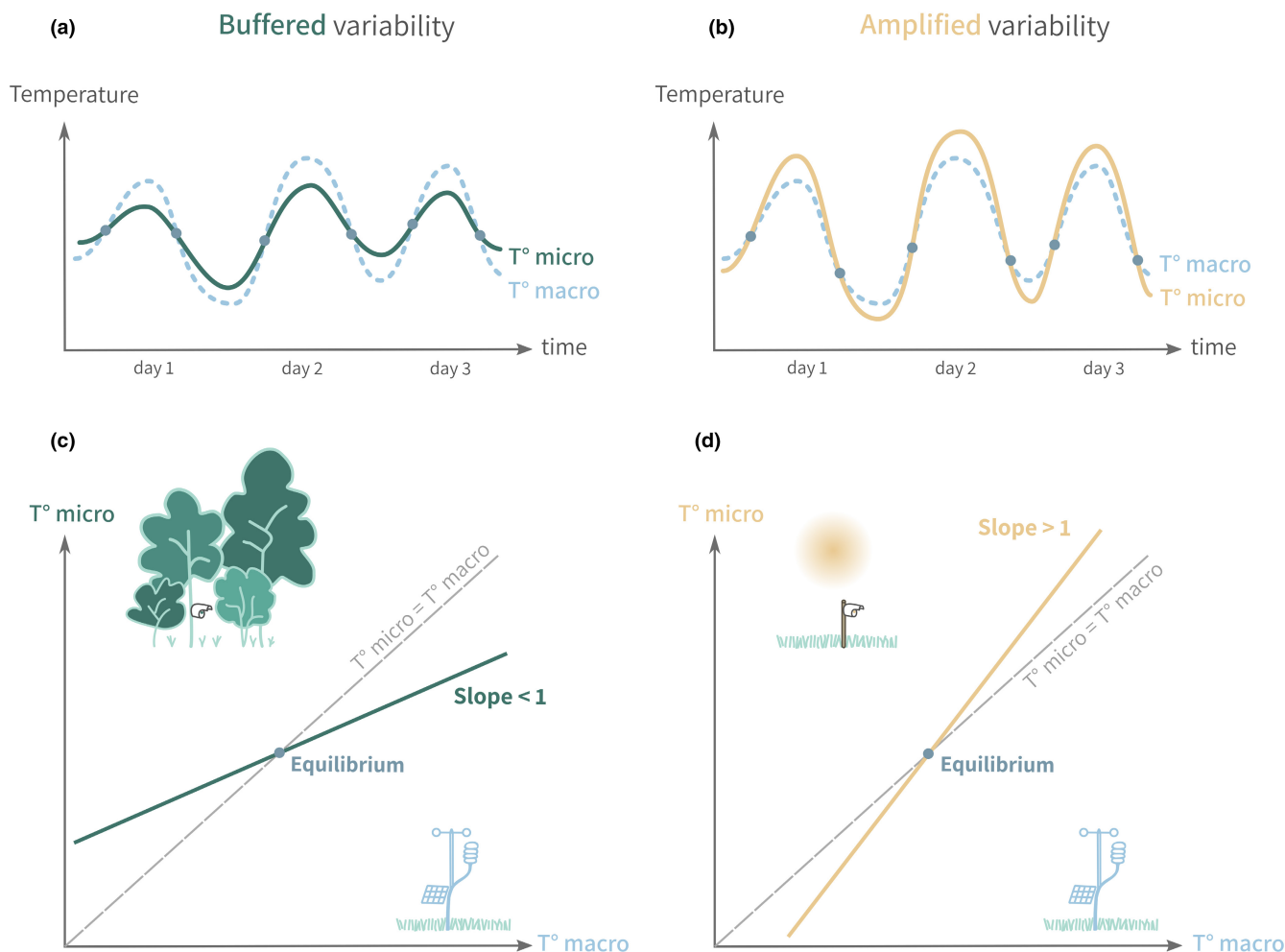


FIGURE 1 (a) A forest understorey where the microclimate (in-situ sensors) temperature variability is buffered relative to macroclimate temperature (standardized weather station); and (b) an open grassland where temperature variability is amplified; (c, d) the slope relating microclimate to macroclimate for these two contrasting habitats, and the equilibrium where microclimate equals macroclimate (dots), at a daily level (a, b) or mean level over weeks or months, where the regression line crosses the identity line (c, d).

shift along seasonal trends (e.g. summer vs winter or along months) and macroclimatic gradient (e.g. latitude or altitude) in temperature, as different spatiotemporal contexts will determine the position of the point cloud linking microclimate to macroclimate (Figure S0). Therefore, the mean macroclimate temperature can be used as a predictor of the equilibrium. The slope and mean equilibrium can be calculated at any chosen temporal resolution, for example, weeks or months.

In brief, the slope and equilibrium approach aims at reconstructing microclimatic patterns, from relevant local drivers of the buffering or amplifying capacity of the habitat and from macroclimate data that are readily available worldwide. We provide a general framework that should be applicable to any kind of microclimate, although we call for more extensive testing of the method on diverse habitats, and we illustrate the approach by focusing on two common habitats with 1 year of hourly temperature measurements. We used a paired design of sensors in open grasslands and forest understoreys (microclimate) across 13 sites equipped with standardized weather stations (macroclimate), covering a wide climatic gradient in France

(Figure 2). We hypothesize that (i) the slope of the linear relationship between macroclimate and microclimate will be smaller than 1 for sensors in forest understoreys, due to the buffering effect of the canopy, but higher than 1 for sensors located in open grasslands because they are located above vegetation and closer to the surface than weather stations; (ii) the slope will be determined by local environment characteristics, and will depend on the leaf-on vs leaf-off period for broadleaf forest stands, but not for coniferous forest stands and (iii) the equilibrium will depend primarily on average macroclimate conditions irrespective of the habitat (open vs forest) and the local stand characteristics within forest understoreys.

2 | MATERIALS AND METHODS

2.1 | Study area and sampling design

Our study sites belong to the French network of permanent forest plots for the long-term monitoring of forest ecosystems

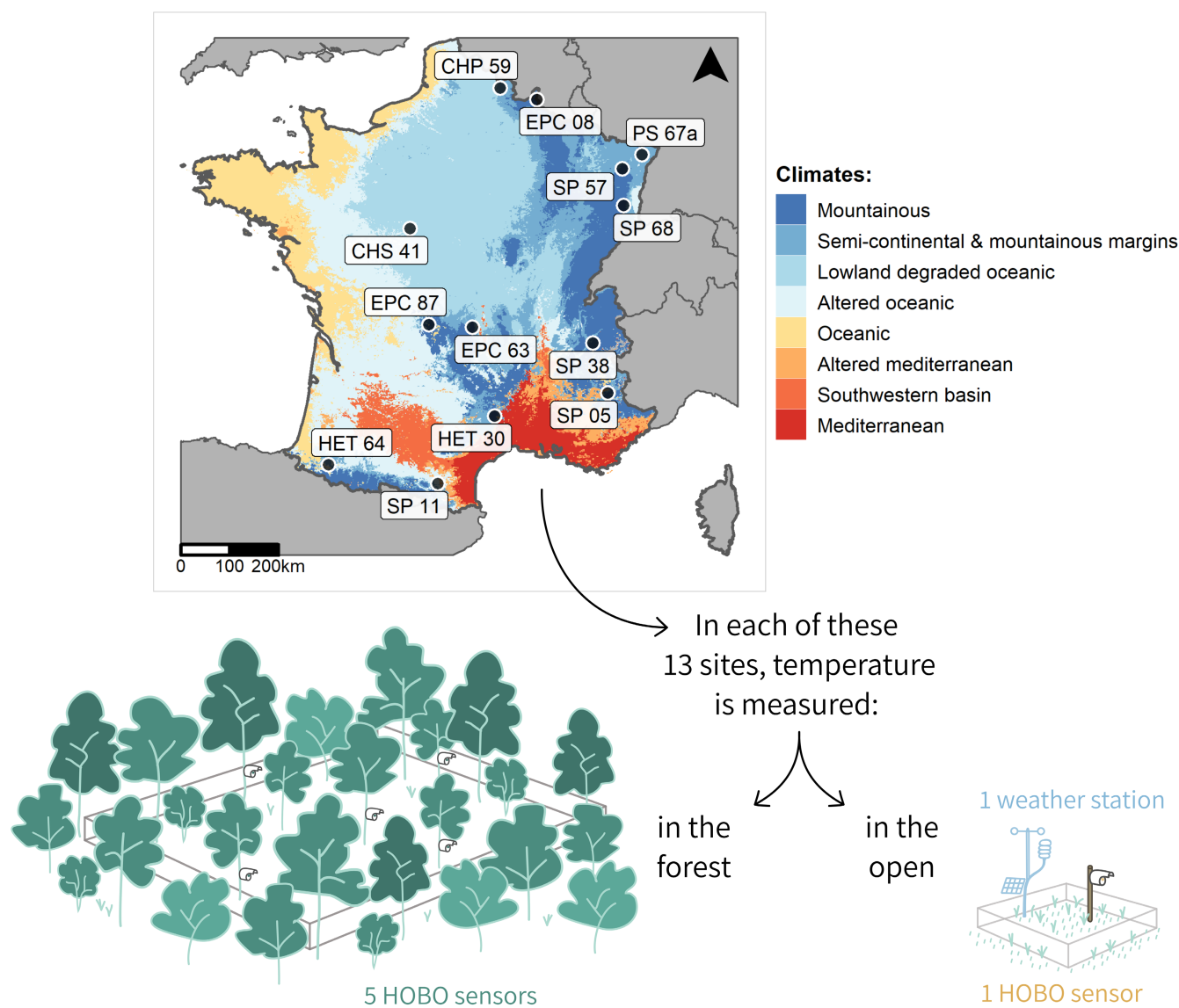


FIGURE 2 A paired sampling design of open grasslands vs forest understoreys equipped with HOBO microclimate temperature sensors. In each of the 13 sites, 5 sensors are set up within a 0.5-ha forest plot (one on each side plus one in the centre), and a sixth is located next to the forest, in an open grassland with a standardized weather station (the macroclimate temperature reference). Sites are located in different climates, following the French classification from Joly et al. (2010). Each site is labelled according to the dominant tree species in the forest plot: HET = *Fagus sylvatica* (Beech); CHP/CHS = *Quercus robur* and *Q. petraea* (Oak); PS = *Pinus sylvestris* (Pine); SP = *Abies alba* (Fir) and EPC = *Picea abies* (Spruce).

(RENECOFOR: <http://www1.onf.fr/renecofor>), with 102 plots located in public, productive forests managed by the French forest office (ONF) following standard regional silvicultural management practices (Ulrich, 1995). We focused on 13 of those sites benefiting from a strictly paired design of open vs forest habitats, where free-air temperature conditions are available from a standardized weather station in fully open conditions next to the forest. Each forest plot is made of a central fenced area of 0.5 ha (Boulanger et al., 2018). Collectively, the 13 sites span a wide range of conditions, with an elevation ranging from 127 to 1400m above sea level (Table S1), and a selection of common temperate trees species, with both broadleaf- ($n = 4$) and conifer- ($n = 9$) dominated stands (Figure 2).

2.2 | Measuring microclimate and macroclimate

Solar radiation is highly variable under forest canopies, generating strong spatiotemporal variation in forest microclimates (Reifsnnyder et al., 1971). We thus measured sub-canopy hourly temperature in each of the 13 forests by installing five temperature sensors 25–60m apart within the 0.5-ha fenced plot (Figure 2). Another temperature sensor was installed in the paired open plot, located 0.5–4 km away (Table S1), a grassland also equipped with a standardized weather station measuring temperature at 1.5 m. We used Onset® HOBO® Pendant data loggers UA-001-08, measuring temperature from -20 to $+70^{\circ}\text{C}$ with a manufacturer-reported accuracy of $\pm 0.53^{\circ}\text{C}$. All sensors were set 1 m above ground on a tree trunk or wooden pole (Figure S1). To minimize

overheating due to the exposure to direct solar radiation, they were oriented northward and hung by a hook inside white homemade PVC shields (10 × 15 cm), in a similar design to Zellweger et al. (2019).

For all our 78 HOBO sensors as well as the 13 standardized weather stations, we collected hourly temperature records during one complete year, from April 21st 2018 to April 20th 2019. After computing hourly standard deviation for the five sensors located in each forest plot (Figure S2) and visually checking the distribution of the raw temperature records (Figures S3 and S4), two records (hourly outliers from a single site) were detected and removed before further analysis because of their incoherence with the time series, probably resulting from sensor malfunction. Since our reference plots in open areas were not necessarily located at the exact same elevation as the forest plots (Table S1), we applied a correction to each of the forest temperature time series, using an adiabatic lapse rate of $-0.56^{\circ}\text{C}/100\text{m}$ (Rolland, 2003).

2.3 | Calculating the slope and equilibrium

To account for the seasonal change in canopy cover, we distinguished two phenological periods for all sites: leaf-off (December–April) and leaf-on (May–November). Although this distinction chiefly makes sense for deciduous forests, we used it systematically in this study for its straightforward meaning.

For each of the 78 HOBO sensors (65 in forests and 13 in open grasslands), we fitted two separate linear mixed-effects models (LMMs) for the leaf-on and leaf-off period, linking the hourly records from the focal sensor to the corresponding records from the paired weather station. To account for seasonal changes similarly to common practice using monthly offsets, and although other time periods (such as weeks) could have been chosen, we calculated the mean equilibrium at the month level. We thus added the month as a random intercept term in our 156 LMMs (i.e. one for each sensor and period), 'Month' being a factor with seven and five levels for leaf-on and off, respectively. The slope estimate was extracted from each LMM, and the equilibrium was calculated for each month and for each sensor using the formula: $\text{equilibrium} = \text{intercept}/(1 - \text{slope})$ (see the Supplement Information for an explanation of how this formula was derived).

All steps of data exploration, preparation and visualization were performed in R version 4.1.2 (R Core Team, 2021), using the TIDYVERSE and LUBRDATE packages (Grolemund & Wickham, 2011; Wickham et al., 2019). We used the LME4 package (Bates et al., 2015) to calculate and extract the slope and equilibrium (see 'Data availability' for the full RMarkdown report).

2.4 | Compiling predictors for the slope and equilibrium

In addition to testing the effects of habitat (forest vs open), period (leaf-on vs leaf-off) and stand type (broadleaf vs conifer) on the

variability of the slope and equilibrium parameters, we gathered predictors potentially related to the spatiotemporal variation in macroclimate and microclimate conditions. To avoid multicollinearity, we excluded candidate predictors for which Pearson's correlation coefficient exceeded 0.7.

As equilibrium was calculated at a monthly scale, we computed the mean monthly macroclimate temperature for each of the 13 sites, using weather station records between April 2018 and April 2019.

For each weather station in the open, the height of, and distance to the nearest edge (forest or hedgerow) were compiled (Table S2).

For each of the 13 forest plots, stand age (years) was estimated from dendrochronological series extracted from dominant trees in 1995 (Lebourgeois et al., 2010). Mean tree height (m) at the stand level was calculated from a set of 70–201 individual tree heights measured per plot in 2014. Dendrometric inventories were conducted in 2019, providing further stand descriptors: basal area ($\text{m}^2 \cdot \text{ha}^{-1}$); mean diameter at breast height (cm) and stem density (per hectare). The shade-casting ability (SCA) index, ranging from 1 for very low to 5 for very high SCA, was retrieved for each tree species (Käber et al., 2021; Vanneste et al., 2020). We computed the mean SCA of all overstorey trees (defined as trees higher than the base of dominant or codominant tree crowns), representing 62–543 trees per plot (Table S3).

The percentage of vegetation cover was visually assessed during the leaf-on period in 2015 at the sensor level for the four peripheral sensors, and for each vertical stratum separately: low shrubs (woody plants of 0.3–2 m), high shrubs (2–7 m) and trees (>7 m). For the central sensor, we computed the mean cover of these four sensors (Table S4).

2.5 | Modelling the slope and equilibrium

Slope and equilibrium were modelled separately as response variables. To assess their main determinants, we operated in two steps: first we considered all sensors to test the effect of open vs forest, then we focused on sensors from a given habitat, using appropriate sets of predictor variables.

We first compared four candidate models to test all combinations of habitat (forest vs open), period (leaf-on vs leaf-off) and their two-way interaction on the spatiotemporal variation of the slope ($n = 156$). We then built a set of simple linear models to check whether height and distance to the nearest forest or hedgerow, interacting or not with the period, could explain the slope in open habitats ($n = 26$). Then, we assessed the explanatory power of local stand and cover characteristics on the slope for forest habitats ($n = 130$). We excluded diameter which was correlated with two other predictors (Figure S8). Basal area, SCA, age, height, stem density, cover of trees, high and low shrubs as well as stand type (broadleaf vs conifer) were used as predictors interacting with the period to build a 'full' model (Zuur et al., 2009). We used a backward elimination strategy with *F*-tests to generate a simplified model.

The plots PS67a and HET30 had a slope very close to one, and consequently had a high dispersion of their monthly equilibrium, extending

outside the distribution of measured temperatures, as low as -589.1°C for PS67a in July to $+533.5^{\circ}\text{C}$ for HET30 in January. Because of the extreme values reached, these two problematic plots had to be removed from equilibrium modelling to explain any variation at all. The equilibrium ($n = 792$ without HET30 and PS67a) was computed for each month, so we first tested a set of all combinations of monthly mean temperature, habitat and their two-way interaction on the spatiotemporal variation of the equilibrium. We then assessed the explanatory power of local stand characteristics, in addition to monthly mean temperature (checking again for potential correlations beforehand), on the equilibrium for forests only ($n = 780$). Starting from this full model, we again generated a simplified candidate model using a backward elimination strategy.

We used LMMs with site ID (13 levels) as a random intercept term to account for the nested sampling design, except for candidate models of the slope in the open (no replicate per site), for which we used simple linear models. During model selection, we used maximum likelihood (ML) instead of restricted maximum likelihood (REML) to compare models with different fixed effects (Zuur et al., 2009). For the backward elimination, we used the *step* function from the *LMERTEST* package (Kuznetsova et al., 2017). To select the best model, we computed the second-order Akaike information criterion (AICc). Once the best model was selected, we reran it using REML instead of ML, to generate more accurate coefficient estimates. To assess the relative importance of each predictor variable, we standardized each quantitative predictor with *gscale* from the *JTOOLS* package (Long, 2020), suitable for situations with quantitative and binary qualitative parameters. We computed the marginal and conditional R^2 using *r.squaredGLMM* from the *MuMIn* package (Bartoń, 2013), respectively representing the percentage of variation explained by fixed effects only, and both fixed and random effects. We used *tab_model* from the *sjPlot* package (Lüdtke, 2021) to print model parameters, and *ggpredict* from the *GGEFFECTS* package (Lüdtke, 2018) to plot model predictions.

3 | RESULTS

We found hourly temperature records measured by HOBO sensors to be linearly related to the corresponding records from weather stations (Figure 3, Figure S6), with marginal R^2 ranging from 80% to 98% (conditional R^2 : 89%–99%) during the leaf-on, and from 77% to 97% (conditional R^2 : 81%–97%) during the leaf-off period. After extracting the slope and equilibrium parameters, we found a mean slope of 0.88 (range = 0.66–1.23) and a monthly equilibrium ranging from 4.1° in January to 12.4°C in September, after removing the two outlier plots HET30 and PS67a.

3.1 | Modelling the slope

We first modelled all slopes at once, and the interaction between the leaf-on/off period and habitat was selected (R^2 marginal = 58%, Table S5, Figure S7), so we then focused on each habitat separately.

For the open habitat, HOBO sensors compared to weather stations always had a slope greater than one, corresponding to an amplified variability in temperature (Figure 3). The slope ranged from 1.05 to 1.23 across our 13 open habitats, with a mean and median of 1.13 ± 0.05 . In contrast, most slopes in forests were lower than one, with a mean of 0.83 ± 0.1 . The minimum slope was 0.66 for SP57 during the leaf-on period, while HET30 and PS67a had slopes very close to one and up to 1.04.

For slopes in the open, our best model included only the period (R^2 marginal = 55%, Table S6), although we had another competitive model (delta AICc < 2) with also an independent effect of the height of the nearest edge. But this predictor had a negligible and insignificant effect, so we chose the simpler model with only the period. The slope was estimated at 1.16 during the leaf-on period (95% CI = 1.14–1.18) and 1.09 during the leaf-off period (95% CI = 1.06–1.12).

For slopes in forests, the selected model involved the period in interaction with the dominant tree type (broadleaf vs conifer), SCA, age, height, stem density, cover of the low shrub stratum, and without an interaction, cover of the high shrub stratum (marginal $R^2 = 56\%$). Slopes were significantly lower during the leaf-on period (0.73) than the leaf-off period (0.87) in broadleaf plots (Figures 3 and 4, Figures S6 and S7). In coniferous plots, it was intermediate and not affected by the period (0.85 and 0.84). The mean SCA and stem density had a pronounced negative impact on the slope (coefficients of -0.10 and -0.09). Canopy height had the greatest effect on slope, with a more negative impact during the leaf-on period (-0.15). The cover of the higher and lower shrub strata had a slight, negative effect on slopes, during the leaf-on but not the leaf-off period for the latter. Age was the only quantitative predictor with a positive effect: older forest plots had a higher slope than younger ones (Figure 4, Figure S9, Table S7).

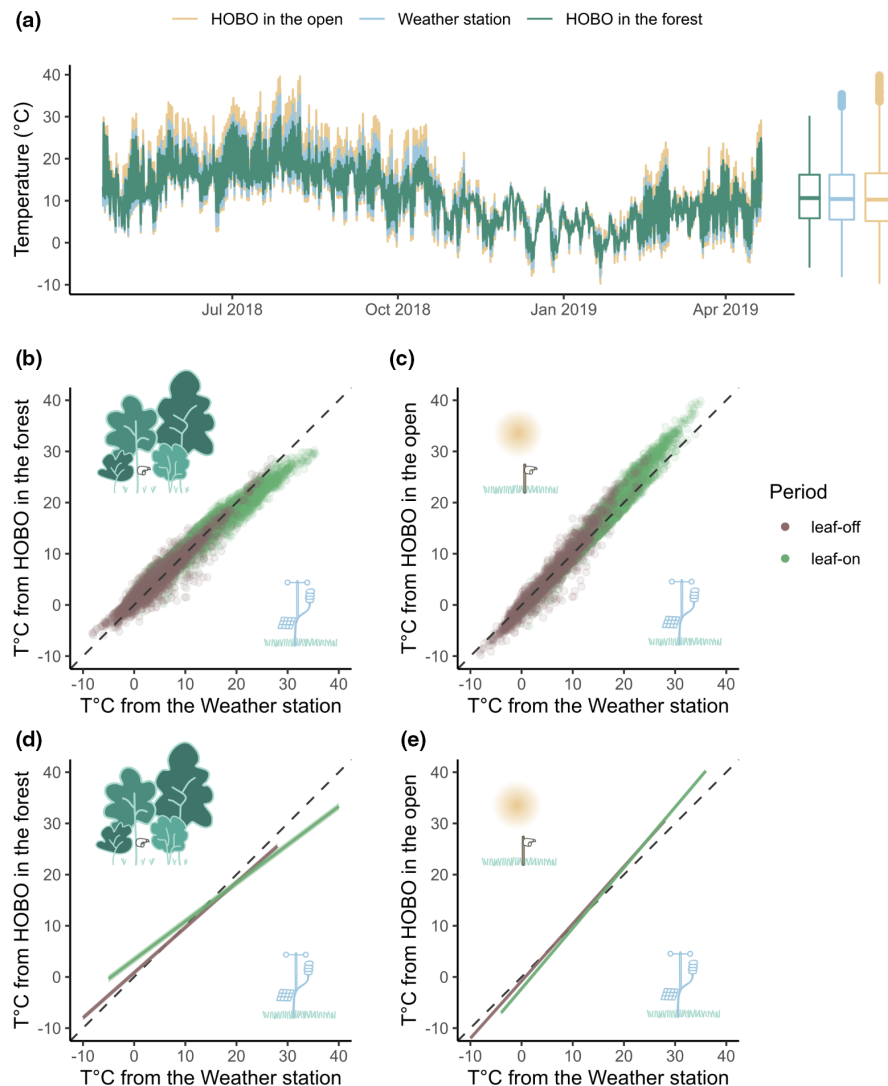
3.2 | Modelling the equilibrium

Mean monthly macroclimate temperature explained a great proportion of the variance in equilibrium, in interaction with the habitat ($n = 792$, R^2 marginal = 47%; Figure 5, Table S8). When modelling equilibrium in forest plots only, adding stand variables did not significantly improve the model. Instead, monthly mean macroclimate temperature, that is, temperatures measured at the level of weather stations, was the only variable selected in a backward elimination of fixed effects.

4 | DISCUSSION

The slope and equilibrium are two simple parameters describing the linear relationship between microclimate and macroclimate. As hypothesized, hourly temperatures had an amplified variability (slope > 1; amplifying effect) in all open habitats compared to the reference weather stations, and a buffered variability (slope < 1;

FIGURE 3 Applying the 'slope and equilibrium' approach to the CHP59 site: (a) temperature time series measured by the HOBO sensor at the central position in the forest plot (the measurements from the four other sensors are not displayed here, but exhibit similar patterns), the paired weather station and the HOBO sensor beside it in the open, with a boxplot showing temperature ranges at a yearly level; (b) relating macroclimate (weather station) to microclimate temperature measured hourly by HOBO sensors, in the forest and (c) in the open; (d and e) resulting linear relationships and their respective 95% confidence interval, which here cannot be distinguished from the regression lines, as they are very close to each other. The equilibrium is then calculated for each month with the leaf-on slope from May to November, and with the leaf-off slope from December to April.



buffering effect) in most forest habitats. Consistent with the hypotheses as well, the phenological period had a major influence on the slope in broadleaf stands but also in open grasslands; local forest structure and cover were the main drivers of the slope in forest understoreys, while the equilibrium depended instead on mean macroclimate temperatures. The slope and equilibrium method can be applied on any temporal resolution and any habitat to reconstruct microclimate temperature from macroclimate.

4.1 | Slope in forests: The buffering effect

Metrics related to forest structure and cover explained a majority of the variance in forest slopes, together with the phenological leaf-on or leaf-off period (Figure 4). Here, slopes were considered constant within each phenological period, but with more extensive datasets, slopes could also be computed and modelled at a finer temporal resolution, for instance to investigate the relationship with local soil water status (Davis, Dobrowski, et al., 2019; McLaughlin et al., 2017). Different seasons may involve distinct

sets of microclimate predictors (Greiser et al., 2018). As postulated in our second hypothesis and consistent with former findings (von Arx et al., 2012), we show that the leaf-off and leaf-on periods were very contrasting for most broadleaf forests, but less so for conifer-dominated stands. More precise phenological dates of leafing and leaf shedding for each location could improve the precision of the model, albeit we already obtained convincing results with this crude splitting of months, allowing a consistent comparison across sites (von Arx et al., 2012). Importantly, our findings suggest that the period interacts with most predictors selected in our best model, usually with a more pronounced effect during leaf-on.

This was especially the case for stand height, which among our continuous predictors had the strongest effect on slope, consistent with former findings suggesting that maximum temperatures are driven by canopy height (Fridley, 2009; Vanneste et al., 2020). Forest age actually had a counterintuitive, positive effect on the slope such that older forests had a weaker buffering effect. Mature, older forests usually have taller and more structurally complex canopies, providing additional insulating power compared to younger and simpler forest structures (Frey et al., 2016;

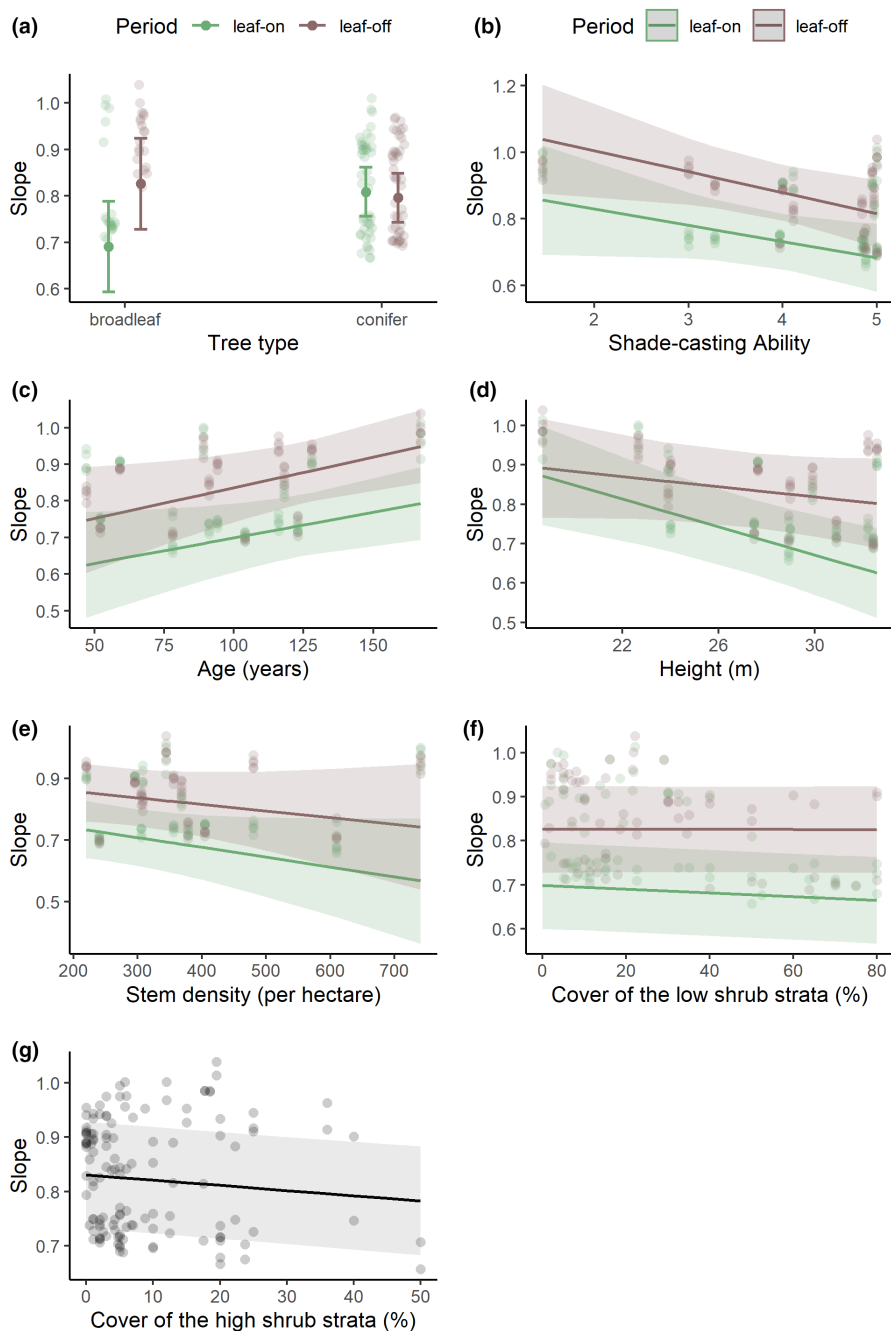


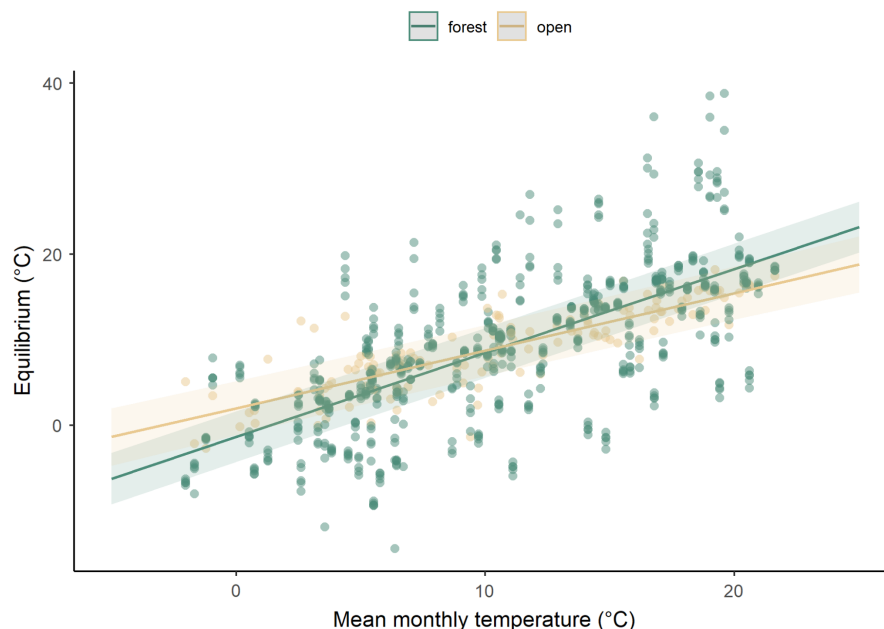
FIGURE 4 Predictions from the best model explaining forest microclimate to macroclimate temperature slopes, with 95% confidence intervals. These eight fixed effects explain 56% of the slope variance (see [Table S7](#) for model parameters and estimates). The first six predictors interact with the period (leaf-on in green vs leaf-off in brown), while the last one has an independent effect on slope (predictions are plotted for the leaf-off period). Other factors are here held constant at their median, and considering a broadleaf tree type for (b–g; see [Figure S9](#) for this figure, with the reference set to conifer).

Lindenmayer et al., 2022). But here, age is not equivalent to maturity, as we are considering only adult and managed forest stands, and hence we do not compare them to young, immature stages. Age is not correlated to height or mean diameter in our sampling, as we also compare trees with drastically different growth rates (e.g. *Picea abies* versus *Quercus robur*) and pedoclimatic conditions (e.g. rich lowland versus acidic mountain). Interestingly, tree canopy cover, a common proxy for microclimate temperature (Zellweger et al., 2020), was not included in our best model, contrary to shrub cover. The low shrub stratum (0.3–2 m) only had an impact during the leaf-on period, whereas the impact of the high shrub stratum (2–7 m) was independent from the period, suggesting that even with shed leaves, high shrubs can still act as an insulating

layer. This is in accordance with recent publications emphasizing the role of the understorey layer (Kovács et al., 2017; Stickley & Fraterrigo, 2021). Finally, although a simple five-scale index, the stand SCA had a complementary positive effect on buffering, by integrating species-specific traits such as leaf size, angle, density and phenology (Käber et al., 2021). The densely packed branches of *Abies alba* may buffer temperature much more than the sparse needles of *Pinus sylvestris*.

Since substantial temperature differences were observed among sensors located within the same 0.5-ha plot, predictions might be further improved by going from stand level to finer-scale predictors, for example using variables derived from light detection and ranging (LiDAR; Davis, Synes, et al., 2019). We should also consider long-term

FIGURE 5 Explaining equilibrium by mean monthly temperature from weather station records, in open and forest habitats (interaction terms in the model). 95% confidence intervals are displayed. These two interacting fixed effects explained 47% of equilibrium variance. Two plots behaved as outliers and were excluded from this model. The estimates are presented in Table S8.



datasets of temperature measurements to confirm the patterns observed, because results could vary from year to year, reflecting weather and not climate (Lembrechts et al., 2019). A nonlinear relationship with microclimate temperature offsets has been found for canopy cover (Ashcroft & Gollan, 2012; Zellweger et al., 2020) or height (Jucker et al., 2018); going beyond linear models could thus improve predictions in future endeavours to explain the slope. Although not tested here, topographic variables, cold air drainage, coastal or riparian effects should influence the slope as well, and may explain part of the residual variance. Canopy and topography indeed have complementary and sometimes interactive effects on microclimate temperature (Ashcroft & Gollan, 2012; Davis, Synes, et al., 2019; Jucker et al., 2018; Zellweger et al., 2019).

4.2 | Slope in the open: The amplifying effect

Hourly temperatures measured by our sensors in open habitats were more variable than the ones measured by the standardized weather stations right beside them, so that the slope was systematically greater than one. Daily maximum temperature records by our low-cost sensors were frequently warmer by several degrees (and vice versa for minimum temperatures) compared to the standardized weather stations, especially during cloud-free conditions. Radiative fluxes dominate near the ground, especially on the layer just on top of the vegetation canopy. This amplifying effect could therefore partly be attributed to the difference in measurement height (1 m for microclimate temperature sensors, versus 1.5 m for weather stations). The very reason of putting standardized weather stations thermometers higher up is to escape these near-ground radiative effect on temperature (WMO, 2018).

Weather stations as a reference are the golden standard, because although they do not represent well the local climatic

conditions close to the ground where most species live (Potter et al., 2013), the parameters they measure can be directly related to all global-scale climatic data currently available. However, it is not always feasible to get data from a neighbouring weather station that can be strictly paired with the microclimate variable at study. Using macroclimate temperature grids at fine temporal resolutions such as ERA5-Land as a reference could be a good substitute, except in the context of regions with marked topographic heterogeneity, for which a different baseline temperature could result in artificial differences with the focal microclimate (Figure S5). Then the use of paired temperature sensors in open conditions as a reference could be recommended. However, we caution scientists who plan to use such low-cost sensors and homemade radiation shields as a 'proxy' for macroclimate temperature reference. Recent studies have warned about the limitations of such equipment, deemed insufficient to prevent overheating during the day: measurements are influenced by the temperature of radiation shields, which absorb solar radiations (Maclean et al., 2021; Terando et al., 2017). The method we describe in this paper could actually represent a way to quantify and emancipate from this bias of amplified variability in temperature records with low-cost sensors, by applying a corrective equation linking them to those of standardized weather stations.

Slopes in the open were only affected by the period, and not significantly by the proximity or height of the nearest edge. Topography or distance to water could be relevant predictors, but were not tested here. Differences between HOBO and weather station temperature were more pronounced during the leaf-on period, with more frequent warm, sunny weather. Other situations are prone to amplified fluctuations of temperature, such as the surface of leaves in the upper forest canopy that accumulate heat during the day, and will also have slopes significantly higher than one (Miller et al., 2021; Pincebourde & Suppo, 2016).

4.3 | Equilibrium, driven by temporal fluctuations in macroclimate

The equilibrium is the temperature at which microclimate equals macroclimate. Microclimate temperatures tend to oscillate around the mean macroclimate temperature of the region. We observed a slightly different relationship linking the equilibrium to mean temperature between habitats, with equilibrium increasing more rapidly in forests than in open habitats, although the difference was too small to infer a specific mechanism at work. The difference in the variability of equilibria between forests and grasslands may have caused this effect, since we only had a single replicate in the open for each site, located right near the weather station. Therefore, studies encompassing more open habitats are needed to confirm whether this result can be replicated and explained. Our findings suggest that the equilibrium is rather independent of stand characteristics in forests, depending only on this mean temperature as measured by standardized weather stations. Deriving the equilibrium is therefore rather straightforward, as mean temperatures are readily available at the global extent from large-scale temperature grids.

In the case of slope values that are very close to one between macroclimate and microclimate temperature, the equilibrium may however lose its meaning, as observed here for a lowland forest stand of *Pinus sylvestris* (PS67a) and a mountainous forest stand of *Fagus sylvatica* (HET30). The equilibrium can then reach very unrealistic temperatures, or may even theoretically never be reached if microclimate is systematically warmer or colder than macroclimate. HET30 is our oldest forest stand (167 years) and yet it has the lowest canopy (19 m) because of the harsh environmental conditions, being also the only one exposed to South-East and the highest in altitude (1400 m). PS67a is our only *Pinus sylvestris* stand, with the lowest level of canopy cover and SCA index (1.45 on a scale of 1 to 5). These specificities could explain the fact that forest microclimate in these two stands is tightly coupled to macroclimate, without a perceptible buffering effect. In the case of a slope very close to one (more research is needed for a precise threshold, but we suggest ± 0.02 , e.g. 1.001) and if the intercept is close to zero, we suggest the equilibrium should not be modelled, as the value per se may have no biophysical meaning. In such situations, we should consider microclimate temperature to be similar to macroclimate. The equilibrium is otherwise needed to reconstruct microclimate temperature from its linear relationship to macroclimate, as we need the intercept parameter as well as the slope: $\text{intercept} = \text{equilibrium} \times (1 - \text{slope})$.

4.4 | Slope and equilibrium, two parameters to rule microclimate

The huge variation in offsets over months, days and hours within a given habitat or microhabitat is like a noise masking the signal of forest buffering. Rather than just focusing on an additive effect causing temperature to increase or decrease at a given moment in time, the slope and equilibrium approach places emphasis on microclimate

stability, or magnitude of change over time, independently from the temporal resolution. Hence, a serious advantage of this method is its flexibility: it can be used similarly for any temporal resolution, that is, daily averages as well as sub-hourly data, and we can therefore make full use of meteorological time series at high temporal resolution. It could also potentially be applied to other relevant climatic variable such as relative humidity or vapour pressure deficit (Davis, Dobrowski, et al., 2019). This modelling approach allows us to clearly dissociate temporal macroscale drivers (equilibrium) from stand characteristics, vegetation cover or other appropriate local drivers (slope). We can thus focus on the buffering process itself, and not the offsets arising therefrom—from this method, offsets can easily be calculated with the following formula (see the [Supplement Information](#) for details on how this formula was derived): $\text{offset} (T_{\text{micro}} - T_{\text{macro}}) = \text{equilibrium} \times (1 - \text{slope}) + T_{\text{macro}} \times (\text{slope} - 1)$.

For instance, with forest understorey, if climate change results in a 1°C increase in mean monthly temperatures, this will affect the equilibrium. However, if rainfall or land use change also result in changing canopy cover, then this will affect the buffering capacity of the forest and hence the slope of the relationship between macroclimate and microclimate temperature (De Frenne et al., 2021). This suggests that despite a likely shift in equilibrium induced by climate change, forest management strategies can still be deployed to conserve if not adjust the slope to maintain a favourable temperature for understorey species. The method represents a way to capture these complex interactions in a manner that cannot be accomplished by modelling offsets directly. This approach thus represents a conceptual advance, and a way forward to reduce the number of models needed to model microclimate from macroclimate. We encourage biogeographers and ecologists using statistical models of microclimate to go from the rigid and time-consuming approach of modelling each climatic offset to a more indicative and flexible method: the slope and equilibrium approach.

AUTHOR CONTRIBUTIONS

Fabien Spicher and Jonathan Lenoir, with the help of Benoit Richard, Guillaume Decocq and Manuel Nicolas, designed and conducted the experiment; Eva Gril performed the analyses with Jonathan Lenoir, Fabien Spicher and Ronan Marrec; Eva Gril wrote the paper with major inputs from Jonathan Lenoir, Michael B. Ashcroft, Ronan Marrec, Sylvie Durrieu, Sylvain Pincebourde and Caroline Greiser; Michael B. Ashcroft, Caroline Greiser and Jonathan Lenoir conceived the original idea behind the slope and equilibrium approach.

ACKNOWLEDGEMENTS

We thank Rebecca Senior and another anonymous reviewer, for improving our paper with their insightful feedback. Our full appreciation goes to the ONF site managers, as well as Sébastien Cecchini and Sébastien Macé, from the French network of permanent forest plots for the long-term monitoring of forest ecosystems (RENECOFOR). We deeply thank Emilie Gallet-Moron, who contributed to data

compiling. J.L. acknowledges funding from the Centre National de la Recherche Scientifique (CNRS), under the framework of the Mission pour les Initiatives Transverses et Interdisciplinaires (MITI, Défi INFINITI 2018: MORFO project) and the Agence Nationale de la Recherche (ANR), under the framework of the young investigators' funding scheme (JCJC Grant N°ANR-19-CE32-0005-01: IMPRINT project).

CONFLICT OF INTEREST

The authors have no conflict of interest to declare.

PEER REVIEW

The peer review history for this article is available at <https://www.webofscience.com/api/gateway/wos/peer-review/10.1111/2041-210X.14048>.

DATA AVAILABILITY STATEMENT

The R Markdown script and data are available online on Figshare <https://doi.org/10.6084/m9.figshare.19868101>.

ORCID

Eva Gril  <https://orcid.org/0000-0002-7340-8264>

Fabien Spicher  <https://orcid.org/0000-0002-9999-955X>

Caroline Greiser  <https://orcid.org/0000-0003-4023-4402>

Michael B. Ashcroft  <https://orcid.org/0000-0003-2157-5965>

Sylvain Pincebourde  <https://orcid.org/0000-0001-7964-5861>

Sylvie Durrieu  <https://orcid.org/0000-0001-6145-9614>

Benoit Richard  <https://orcid.org/0000-0003-4522-027X>

Guillaume Decocq  <https://orcid.org/0000-0001-9262-5873>

Ronan Marrec  <https://orcid.org/0000-0003-1607-4939>

Jonathan Lenoir  <https://orcid.org/0000-0003-0638-9582>

REFERENCES

- Ashcroft, M. B., & Gollan, J. R. (2012). Fine-resolution (25 m) topoclimatic grids of near-surface (5 cm) extreme temperatures and humidities across various habitats in a large (200 × 300 km) and diverse region. *International Journal of Climatology*, 32(14), 2134–2148. <https://doi.org/10.1002/joc.2428>
- Bartoń, K. (2013). MuMIn: Multi-model inference. In *R package version 1.10.0*. <https://cran.r-project.org/web/packages/MuMIn/MuMIn.pdf>
- Bates, D., Mächler, M., Bolker, B., & Walker, S. (2015). Fitting linear mixed-effects models using lme4. *Journal of Statistical Software*, 67, 1–48. <https://doi.org/10.18637/jss.v067.i01>
- Boulanger, V., Dupouey, J.-L., Archaux, F., Badeau, V., Baltzinger, C., Chevalier, R., Corcket, E., Dumas, Y., Forgeard, F., Mârell, A., Montpied, P., Paillet, Y., Picard, J.-F., Saïd, S., & Ulrich, E. (2018). Ungulates increase forest plant species richness to the benefit of non-forest specialists. *Global Change Biology*, 24(2), e485–e495. <https://doi.org/10.1111/gcb.13899>
- Bramer, I., Anderson, B. J., Bennie, J., Bladon, A. J., De Frenne, P., Hemming, D., Hill, R. A., Kearney, M. R., Körner, C., Korstjens, A. H., Lenoir, J., Maclean, I. M. D., Marsh, C. D., Morecroft, M. D., Ohlemüller, R., Slater, H. D., Suggitt, A. J., Zellweger, F., & Gillingham, P. K. (2018). Advances in monitoring and modelling climate at ecologically relevant scales. In D. A. Bohan, A. J. Dumbrell, G. Woodward, & M. Jackson (Eds.), *Advances in ecological research* (Vol. 58, pp. 101–161). Academic Press. <https://doi.org/10.1016/b.s.aecr.2017.12.005>
- Davis, F. W., Synes, N. W., Fricker, G. A., McCullough, I. M., Serra-Diaz, J. M., Franklin, J., & Flint, A. L. (2019). LiDAR-derived topography and forest structure predict fine-scale variation in daily surface temperatures in oak savanna and conifer forest landscapes. *Agricultural and Forest Meteorology*, 269–270, 192–202. <https://doi.org/10.1016/j.agrformet.2019.02.015>
- Davis, K. T., Dobrowski, S. Z., Holden, Z. A., Higuera, P. E., & Abatzoglou, J. T. (2019). Microclimatic buffering in forests of the future: The role of local water balance. *Ecography*, 42(1), 1–11. <https://doi.org/10.1111/ecog.03836>
- De Frenne, P., Lenoir, J., Luoto, M., Scheffers, B. R., Zellweger, F., Aalto, J., Ashcroft, M. B., Christiansen, D. M., Decocq, G., Pauw, K. D., Govaert, S., Greiser, C., Gril, E., Hampe, A., Jucker, T., Klimes, D. H., Koelemeijer, I. A., Lembrechts, J. J., Marrec, R., ... Hylander, K. (2021). Forest microclimates and climate change: Importance, drivers and future research agenda. *Global Change Biology*, 27(11), 2279–2297. <https://doi.org/10.1111/gcb.15569>
- Fick, S. E., & Hijmans, R. J. (2017). WorldClim 2: New 1-km spatial resolution climate surfaces for global land areas. *International Journal of Climatology*, 37(12), 4302–4315. <https://doi.org/10.1002/joc.5086>
- Frey, S. J. K., Hadley, A. S., Johnson, S. L., Schulze, M., Jones, J. A., & Betts, M. G. (2016). Spatial models reveal the microclimatic buffering capacity of old-growth forests. *Science Advances*, 2(4), e1501392. <https://doi.org/10.1126/sciadv.1501392>
- Fridley, J. D. (2009). Downscaling climate over complex terrain: High Finescale (<1000 m) spatial variation of near-ground temperatures in a montane forested landscape (Great Smoky Mountains). *Journal of Applied Meteorology and Climatology*, 48(5), 1033–1049. <https://doi.org/10.1175/2008JAMC2084.1>
- Geiger, R., Aron, R. H., & Todhunter, P. (2003). *The climate near the ground*. Rowman & Littlefield.
- Greiser, C., Meineri, E., Luoto, M., Ehrlén, J., & Hylander, K. (2018). Monthly microclimate models in a managed boreal forest landscape. *Agricultural and Forest Meteorology*, 250–251, 147–158. <https://doi.org/10.1016/j.agrformet.2017.12.252>
- Grolemund, G., & Wickham, H. (2011). Dates and times made easy with lubridate. *Journal of Statistical Software*, 40, 1–25. <https://doi.org/10.18637/jss.v040.i03>
- Haesen, S., Lembrechts, J. J., De Frenne, P., Lenoir, J., Aalto, J., Ashcroft, M. B., Kopecký, M., Luoto, M., Maclean, I., Nijs, I., Niittynen, P., van den Hoogen, J., Arriga, N., Bruna, J., Buchmann, N., Čiliak, M., Collalti, A., De Lombaerde, E., Descombes, P., ... Van Meerbeek, K. (2021). ForestTemp – Sub-canopy microclimate temperatures of European forests. *Global Change Biology*, 27(23), 6307–6319. <https://doi.org/10.1111/gcb.15892>
- Humboldt, A. v., & Bonpland, A. (1805). *Essai sur la géographie des plantes, accompagné d'un tableau physique des régions équinoxiales*. <https://gallica.bnf.fr/ark:/12148/bpt6k977938>
- Joly, D., Brossard, T., Cardot, H., Cavailles, J., Hilal, M., & Wavresky, P. (2010). Les types de climats en France, une construction spatiale. *Cybergeo: European Journal of Geography*, 501. <https://doi.org/10.4000/cybergeo.23155>
- Jucker, T., Hardwick, S. R., Both, S., Elias, D. M. O., Ewers, R. M., Milodowski, D. T., Swinfield, T., & Coomes, D. A. (2018). Canopy structure and topography jointly constrain the microclimate of human-modified tropical landscapes. *Global Change Biology*, 24(11), 5243–5258. <https://doi.org/10.1111/gcb.14415>
- Käber, Y., Meyer, P., Stillhard, J., De Lombaerde, E., Zell, J., Stadelmann, G., Bugmann, H., & Bigler, C. (2021). Tree recruitment is determined by stand structure and shade tolerance with uncertain role of climate and water relations. *Ecology and Evolution*, 11(17), 12182–12203. <https://doi.org/10.1002/ece3.7984>

- Kearney, M. R., Gillingham, P. K., Bramer, I., Duffy, J. P., & Maclean, I. M. D. (2020). A method for computing hourly, historical, terrain-corrected microclimate anywhere on earth. *Methods in Ecology and Evolution*, 11(1), 38–43. <https://doi.org/10.1111/2041-210X.13330>
- Kovács, B., Tinya, F., & Ódor, P. (2017). Stand structural drivers of microclimate in mature temperate mixed forests. *Agricultural and Forest Meteorology*, 234–235, 11–21. <https://doi.org/10.1016/j.agrformet.2016.11.268>
- Kuznetsova, A., Brockhoff, P. B., & Christensen, R. H. B. (2017). lmerTest package: Tests in linear mixed effects models. *Journal of Statistical Software*, 82, 1–26. <https://doi.org/10.18637/jss.v082.i13>
- Lebourgeois, F., Rathgeber, C., Merian, P., & Ulrich, E. (2010). Sensibilité des écosystèmes forestiers tempérés français à la variabilité climatique et aux événements extrêmes: Exemple du réseau RENECOFOR. *Collection EDYTEM. Cahiers de Géographie*, 11(1), 21–28. <https://doi.org/10.3406/edyte.2010.1141>
- Lembrechts, J. J., Nijs, I., & Lenoir, J. (2019). Incorporating microclimate into species distribution models. *Ecography*, 42(7), 1267–1279. <https://doi.org/10.1111/ecog.03947>
- Lenoir, J., Bertrand, R., Comte, L., Bourgeaud, L., Hattab, T., Muriene, J., & Grenouillet, G. (2020). Species better track climate warming in the oceans than on land. *Nature Ecology & Evolution*, 4(8), 1044–1059. <https://doi.org/10.1038/s41559-020-1198-2>
- Lenoir, J., Hattab, T., & Pierre, G. (2017). Climatic microrefugia under anthropogenic climate change: Implications for species redistribution. *Ecography*, 40(2), 253–266. <https://doi.org/10.1111/ecog.02788>
- Lindenmayer, D., Blanchard, W., McBurney, L., Bowd, E., Youngentob, K., Marsh, K., & Taylor, C. (2022). Stand age related differences in forest microclimate. *Forest Ecology and Management*, 510, 120101. <https://doi.org/10.1016/j.foreco.2022.120101>
- Locosselli, G. M., Cardim, R. H., & Ceccantini, G. (2016). Rock outcrops reduce temperature-induced stress for tropical conifer by decoupling regional climate in the semiarid environment. *International Journal of Biometeorology*, 60(5), 639–649. <https://doi.org/10.1007/s00484-015-1058-y>
- Long, J. A. (2020). *jtools: Analysis and presentation of social scientific data*. <https://cran.r-project.org/package=jtools>
- Lüdtke, D. (2018). Ggeffects: Tidy data frames of marginal effects from regression models. *Journal of Open Source Software*, 3(26), 772. <https://doi.org/10.21105/joss.00772>
- Lüdtke, D. (2021). *sjPlot: Data visualization for statistics in social science*. <https://CRAN.R-project.org/package=sjPlot>
- Maclean, I. M. D., Duffy, J. P., Haesen, S., Govaert, S., Frenne, P. D., Vanneste, T., Lenoir, J., Lembrechts, J. J., Rhodes, M. W., & Meerbeek, K. V. (2021). On the measurement of microclimate. *Methods in Ecology and Evolution*, 12(8), 1397–1410. <https://doi.org/10.1111/2041-210X.13627>
- McLaughlin, B. C., Ackerly, D. D., Klos, P. Z., Natali, J., Dawson, T. E., & Thompson, S. E. (2017). Hydrologic refugia, plants, and climate change. *Global Change Biology*, 23(8), 2941–2961. <https://doi.org/10.1111/gcb.13629>
- Miller, B. D., Carter, K. R., Reed, S. C., Wood, T. E., & Cavaleri, M. A. (2021). Only sun-lit leaves of the uppermost canopy exceed both air temperature and photosynthetic thermal optima in a wet tropical forest. *Agricultural and Forest Meteorology*, 301–302, 108347. <https://doi.org/10.1016/j.agrformet.2021.108347>
- Muñoz-Sabater, J., Dutra, E., Agustí-Panareda, A., Albergel, C., Arduini, G., Balsamo, G., Boussetta, S., Choulga, M., Harrigan, S., Hersbach, H., Martens, B., Miralles, D. G., Piles, M., Rodríguez-Fernández, N. J., Zsoter, E., Buontempo, C., & Thépaut, J.-N. (2021). ERA5-Land: A state-of-the-art global reanalysis dataset for land applications. *Earth System Science Data*, 13(9), 4349–4383. <https://doi.org/10.5194/essd-13-4349-2021>
- Pincebourde, S., & Suppo, C. (2016). The vulnerability of tropical ectotherms to warming is modulated by the microclimatic heterogeneity. *Integrative and Comparative Biology*, 56(1), 85–97. <https://doi.org/10.1093/icb/icw014>
- Potter, K. A., Woods, H. A., & Pincebourde, S. (2013). Microclimatic challenges in global change biology. *Global Change Biology*, 19(10), 2932–2939. <https://doi.org/10.1111/gcb.12257>
- R Core Team. (2021). *R: A language and environment for statistical computing*. R Foundation for Statistical Computing. <https://www.R-project.org/>
- Reifsnnyder, W. E., Furnival, G. M., & Horowitz, J. L. (1971). Spatial and temporal distribution of solar radiation beneath forest canopies. *Agricultural Meteorology*, 9, 21–37. [https://doi.org/10.1016/0002-1571\(71\)90004-5](https://doi.org/10.1016/0002-1571(71)90004-5)
- Rita, A., Bonanomi, G., Allevato, E., Borghetti, M., Cesarano, G., Mogavero, V., Rossi, S., Saulino, L., Zotti, M., & Saracino, A. (2021). Topography modulates near-ground microclimate in the Mediterranean Fagus sylvatica treeline. *Scientific Reports*, 11(1), 8122. <https://doi.org/10.1038/s41598-021-87661-6>
- Rolland, C. (2003). Spatial and seasonal variations of air temperature lapse rates in alpine regions. *Journal of Climate*, 16(7), 1032–1046. [https://doi.org/10.1175/1520-0442\(2003\)016<1032:SASVOA>2.0.CO;2](https://doi.org/10.1175/1520-0442(2003)016<1032:SASVOA>2.0.CO;2)
- Stickley, S. F., & Fraterrigo, J. M. (2021). Understory vegetation contributes to microclimatic buffering of near-surface temperatures in temperate deciduous forests. *Landscape Ecology*, 36, 1197–1213. <https://doi.org/10.1007/s10980-021-01195-w>
- Terando, A. J., Youngsteadt, E., Meineke, E. K., & Prado, S. G. (2017). Ad hoc instrumentation methods in ecological studies produce highly biased temperature measurements. *Ecology and Evolution*, 7(23), 9890–9904. <https://doi.org/10.1002/ece3.3499>
- Ulrich, E. (1995). The renecofor-network: Objectives and realization. *Revue Forestière Française*, 47(2), 107–124. <https://doi.org/10.4267/2042/26634>
- Vanneste, T., Govaert, S., Spicher, F., Brunet, J., Cousins, S. A. O., Decocq, G., Diekmann, M., Graae, B. J., Hedwall, P.-O., Kapás, R. E., Lenoir, J., Liira, J., Lindmo, S., Litza, K., Naaf, T., Orczewska, A., Plue, J., Wulf, M., Verheyen, K., & De Frenne, P. (2020). Contrasting microclimates among hedgerows and woodlands across temperate Europe. *Agricultural and Forest Meteorology*, 281, 107818. <https://doi.org/10.1016/j.agrformet.2019.107818>
- von Arx, G., Dobberty, M., & Rebetez, M. (2012). Spatio-temporal effects of forest canopy on understory microclimate in a long-term experiment in Switzerland. *Agricultural and Forest Meteorology*, 166–167, 144–155. <https://doi.org/10.1016/j.agrformet.2012.07.018>
- Wickham, H., Averick, M., Bryan, J., Chang, W., McGowan, L. D., François, R., Grolemund, G., Hayes, A., Henry, L., Hester, J., Kuhn, M., Pedersen, T. L., Miller, E., Bache, S. M., Müller, K., Ooms, J., Robinson, D., Seidel, D. P., Spinu, V., ... Yutani, H. (2019). Welcome to the Tidyverse. *Journal of Open Source Software*, 4(43), 1686. <https://doi.org/10.21105/joss.01686>
- WMO. (2018). *Guide to instruments and methods of observation* (2018th ed.). World Meteorological Organization.
- Woods, H. A., Pincebourde, S., Dillon, M. E., & Terblanche, J. S. (2021). Extended phenotypes: Buffers or amplifiers of climate change? *Trends in Ecology & Evolution*, 36(10), 889–898. <https://doi.org/10.1016/j.tree.2021.05.010>
- Zellweger, F., Coomes, D., Lenoir, J., Depauw, L., Maes, S. L., Wulf, M., Kirby, K. J., Brunet, J., Kopecký, M., Máliš, F., Schmidt, W., Heinrichs, S., den Ouden, J., Jaroszewicz, B., Buyse, G., Spicher, F., Verheyen, K., & Frenne, P. D. (2019). Seasonal drivers of understory temperature buffering in temperate deciduous forests across Europe. *Global Ecology and Biogeography*, 28(12), 1774–1786. <https://doi.org/10.1111/geb.12991>
- Zellweger, F., Frenne, P. D., Lenoir, J., Vangansbeke, P., Verheyen, K., Bernhardt-Römermann, M., Baeten, L., Hédli, R., Berki, I., Brunet, J., Calster, H. V., Chudomelová, M., Decocq, G., Dirnböck, T., Durak, T., Heinken, T., Jaroszewicz, B., Kopecký, M., Máliš, F., ... Coomes,

D. (2020). Forest microclimate dynamics drive plant responses to warming. *Science*, 368(6492), 772–775. <https://doi.org/10.1126/science.aba6880>

Zuur, A., Ieno, E. N., Walker, N., Saveliev, A. A., & Smith, G. M. (2009). *Mixed effects models and extensions in ecology with R*. Springer Science & Business Media.

SUPPORTING INFORMATION

Additional supporting information can be found online in the Supporting Information section at the end of this article.

How to cite this article: Gril, E., Spicher, F., Greiser, C., Ashcroft, M. B., Pincebourde, S., Durrieu, S., Nicolas, M., Richard, B., Decocq, G., Marrec, R., & Lenoir, J. (2023). Slope and equilibrium: A parsimonious and flexible approach to model microclimate. *Methods in Ecology and Evolution*, 14, 885–897. <https://doi.org/10.1111/2041-210X.14048>